Universe International Journal of Interdisciplinary Research
(Peer Reviewed Refereed Journal)

© UIJIR | ISSN (O) – 2582-6417
MARCH 2022 | Vol. 2 Issue 10
www.uijir.com

ARTIFICIAL INTELLIGENCE SYSTEM FOR CATALOGUING OF COVID-19 FROM CXR IMAGES

Author's Name: Atianashie Miracle A.

Affiliation: Catholic University College of Ghana, Fiapre,Sunyani, Ghana

E-Mail: miracleatianashie81@gmail.com

DOI No. – **08.2020-25662434**

Abstract

Coronavirus Disease 2019 (COVID-19) becomes the crucial disease in recent times. Further, many variants of COVID-19 are evolving from the broad family of severe acute respiratory syndrome (SARS). Thus, the detection of all these variants by using Real-time polymerase chain reaction (RT-PCR) test is a difficult task and time taking. In addition, the conventional methods are failed to classify the COVID-19 in early stage due to complex architecture of chest x-ray (CXR) image. Therefore, this article is focused on implementation of deep learning convolutional neural network (DLCNN) based artificial intelligence approach for classifying COVID-19 disease. Initially, the hybrid features are extracted from CXR dataset by using Multi Block Local Binary Pattern (MB-LBP), and Weber local descriptor (WLD). Further, Increment component analysis (ICA) is used to reduce features, which generates best features. Then, DLCNN model is trained with these features for classification of COVID-19 for each test CXR image. The simulation results show that proposed classification resulted in better subjective and object performance as compared to conventional machine learning and deep learning methods.

Keywords*: Coronavirus, deep learning convolutional neural network, chest x-ray image, Increment component analysis, Weber local descriptor, Multi Block Local Binary Pattern.*

INTRODUCTION

Billions of people have been infected since the COVID-19 epidemic started in Wuhan, China, in December [1]. The virus spread rapidly, generating an epidemic. The virus that caused COVID-19 belongs to a broad family of respiratory viruses that may cause diseases including SARS. The new SARS-CoV-2 virus may cause viral pneumonia. In other states, the mortality rate has risen alarmingly. The death toll is climbing every day, according to the UN. As a result, developing a rapid, accurate, and cost-effective viral pneumonia diagnosis tool is critical. This is the initial step in introducing further preventive measures like as isolation, contact tracking, and treatment to end the pandemic. RT-PCR is a popular approach for identifying viruses using viral nucleic acid detection. [2] This test is quite sensitive and has many flaws. For example, it cannot detect COVID-19 that developed before DNA sequence samples were collected. It also takes 2-3 days to finish and requires various preparations, including public space. Despite their best efforts, many governments are unable to test thousands of individuals in this manner. Continuing this method may impede the pandemic management process. [3].

World Health Organization (WHO) data on COVID-19 prevalence in the most devastated nations is shown in Figure 1. There were 185,039,249 reported diseases in 2000, with the US country itself.

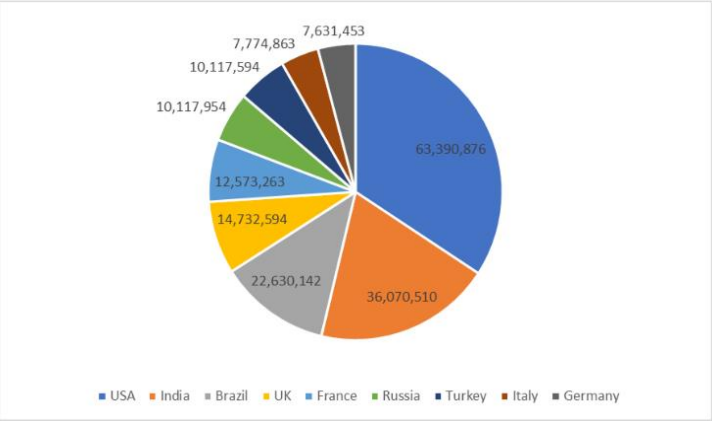

Figure 1. COVID-19 statistics in different countries of year 2021

Various diagnostic tests are also indicated, such as chest ultrasonography, X-rays, MRI, CT, and needle biopsy. Because CT scanning takes longer than CXR images and is not commonly available in many poor countries, CXR images are now extensively used to identify COVID-19 patients. Also, CT scanning is quite costlier, children and pregnant women may be exposed to hazardous quantities of radiation [21]. The availability of X-ray scanning has made it useful in many medical and epidemiological situations [22,23]. CXRs have significant potential for emergency patients and treatment choices because of their quickness, cheap cost, and simplicity. However, prior research found considerable disparities in COVID-19 based CXR images [24].

Although these CNN architectures are well-suited for medical classification applications, the lack of medical data makes training the model difficult. Deep learning models transfers information from a pre-trained dataset including many CXR images to a new dataset. When data is scarce, it's a great way to improve network efficiency and dependability.

Therefore, to overcome the problems of conventional approaches, this article implemented artificial intelligence based DLCNN model classifying COVID-19 disease. Initially, the hybrid features are extracted from CXR dataset by using MB-LBP, and WLD descriptors. Further, ICA is used to reduce features, which generates best features. Then, DLCNN model is trained with these features for classification of COVID-19 for each test CXR image.

Rest of the article is organized as follows: section 2 delas with literature survey with drawbacks. Section 3 deals with the prosed method. Section 4 delas with conclusion and future scope.

LITERATURE SURVEY

This section was created to give an overview of important studies to better understand the issue and present the most current CXR image. CNNs are one of the most successful deep learning models, outperform standard techniques in image and pattern classification [13,14]. It is now employed in medicine, resulting in remarkable outcomes and performance in a range of difficult conditions. [15,16] A number of DL-based medical scanning systems have been developed to help physicians and professionals diagnose, treat, and monitor COVID-19 patients.
The pre-trained ResNet-50 technique is the most efficient, with 98 percent accuracy, 100% specificity, and 96% recall. It is also the most accurate.

In [19] authors utilized the ResNet-18 model as a feature vector to construct meaningful feature representations from CXR images. The collected and inserted attributes formed a multi-layer

perception. A collection of 100 CXR images from 70 patients yielded a 96 percent accuracy rate.

some flaws that need further investigation. For starters, most current systems rely on a limited number of CXR datasets and positive COVID-19 cases, both of which are uncommon. The datasets are too small to accurately reflect the proposed systems' output. Due to a lack of appropriate data.

The greatest results were obtained from VGG19 [12] and MobileNetv2 [13], with accuracy ratings of 0.93 and 0.92.

Sethy et al. [14] devised a hybrid technique using CNN models for feature extraction and SVMs for classification. Using ResNet50 [15] and SVM, they achieved 0.95 accuracy.

a lightweight residual design pattern called PEPX to build their architecture (projection-expansion-projection-extension). An algorithm for understanding COVID-19 indications was also developed.

Farooq et al. [17] use deep CNN to discover COVID-19 and enhance the performance of ResNet-50 [15]. The paper explains the approach in full. At each stage, the input CXR was gradually expanded (128 x 127, 229 x 229, and 224 x 224), and the network was fine-tuned. The authors achieved 0.96 percent accuracy.

According to Hemdan et al., [18], the COVIDX-Net system uses seven CNN models designed by Hemdan. VGG-19 [12] and DenseNet-201 [19] both had 0.90 accuracy.

the consensus of all five radiologists' results of 0.81–0.82. We found DeepCOVID-XR to be more sensitive (0.71) and more specific (0.92) than a single radiologist (0.60) and two radiologists (0.75 and 0.84).

To classify CXR images as COVID-19 or healthy, Chetoui and Akhloufi [25] used EfficientNet-B7 deep CNN to categorise COVID-19 vs healthy. Their analysis included 2385 COVID-19 CXR images from several databases. The recommended approach yielded an ACC.

All of these studies show some fascinating findings. Numerous reasons exist. First, the databases include a few CXR images. Optimisation of hyper-parameters for CNN and Third, examine the CNN architecture's performance. However, little research has been done on how well deep learning algorithms generalise across datasets. Generality is vital in the medical field.

The model for this study was an EfficientNet-B5 that has been fine-tuned based on ImageNet [28] classification performance. They are balanced DCNNs from the EfficientNet family.

The suggested approach's generalisation performance may be improved by testing it on a large number of datasets [36]. Using numerous datasets, we show that the suggested solution outperforms existing algorithms for COVID-19 identification. An explainability model was created and then adjusted to meet the scenario to highlight the COVID-19 and pneumonia signals.

The system was trained on images of healthy persons, pneumonia patients, and COVID-19 patients. The work was restricted by the small dataset of just 285 CXR images used to build a deep learning-based system for COVID-19 prediction.

Working with CXR images, Chowdhury and colleagues [30] created PDCOVIDNet, a parallel-dilated CNN-based framework. Using a dilated convolution in the parallel stack, the authors achieved a detection accuracy of 96.58 percent.

Their approach includes a decomposition method to probe class boundaries for anomalies in the

dataset. It took thousands of CXR images to pre-train the approach to discern key things, and thousands more to re-train it to detect irregularities in CXRs.

El-Rashidy and colleagues [33] created a framework with three layers: patient, cloud, and hospital. The proposed model's accuracy was 99.3% in the final testing phase after preprocessing and data augmentation. Loey et al. [35] employed a dataset of 307 CXR images with four classifications each.

Khalifa and colleagues [40] used deep learning and machine learning to identify the treatment kind and concentration level of COVID-19. The DCNN model was built by converting the data sets' numerical features into visuals. The model's treatment categorization accuracy was 98.05 percent, compared to SVM and DT accuracy. However, the recommended DCNN model performed less correctly (98.2%) than the DT in predicting treatment concentration level (98.5 percent).

The proposed technique has a diagnosis accuracy of 96.75 percent. This strategy improved the Xception model's accuracy by 2.58 percent while minimising the amount of false positives. The authors concluded that their strategy outperformed the COVID-19 method in terms of classification accuracy and diagnostic efficiency. The authors, however, have not compared their results to those of other similar investigations.

Sahlol et al. [42] proposed a superior hybrid classification technique based on CNNs and the marine predator's algorithm. The research included CXR images from international cardiothoracic radiologists. The CXR images were analyzed using CNN's inception design and a swarm-based marine predators' technique to choose the most relevant traits.

However, no fusion approach was used in this work to improve COVID-19 image classification and feature extraction.

PROPOSED METHOD

The key intention of the proposed method is to design a discriminative model for classification. The proposed design of the classification is demonstrated in Figure 2 with four successive steps as preprocessing, feature extraction, feature reduction and classification. Initially, it performs preprocessing to remove noises from COVID-19 region. The noises in the images are removed using the Gaussian filter. The hybrid local descriptors MBLBP and WLD are used to extract the feature invariant discriminative features. The extracted feature causes vast feature space and dimensionality reduction technique is highly significant in reducing the feature vector space. The proposed method develops an advanced MFDA and DLCNN classifier to recognize the COVID-19 from CXR image.

Figure 2. Proposed Block diagram

MB-LBP for Texture Feature Extraction

LBP is conventional texture feature descriptors in computer vision technology. It first divides the image into the cells and then it compares each pixel in the cell with the eight neighbor pixels. A multi-scale blocks LBP descriptor is used to encompass pieces of the CXR image. The texture information is estimated using the reference center pixel value compared with the neighbor 8 pixels. If the neighboring pixel is larger value than the center pixel then it is assigned as 1 or else assigned as 0. In MB-LBP the comparison of pixel value is extended to the sub blocks of image when compared to the point-to-point pixel value comparison in LBP. The MB-LBP feature extraction of

the image is given as follows:

$$MB - LBP\ (D_n) = \sum_{m=0}^{p-1} S(D_m - D_n).2^m$$

$$MB - LBP\ (D_n) = \sum_{m=0}^{p-1} S(T)$$

Here, Dm, Dn m=0,1,…,p-1 which is the gray level of center and surrounding pixel in the CXR image. Dm represents the average sum of the neighborhood values and Dn represents the average sum of the center blocks in the image. $S(T)$ is expressed as follows:

$$S(T) = \begin{cases} 0 & T < 0 \\ 1 & T \geq 0 \end{cases}$$

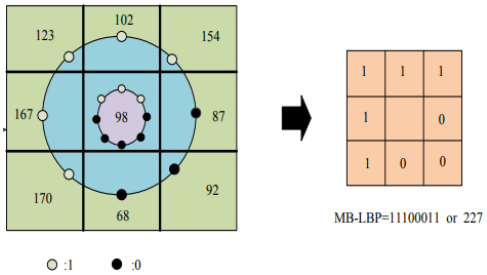

Figure 3. MB-LBP feature extraction process

Figure3 illustrates the 3*3 MB-LBP coding pixels of the given CXR image. The center pixel gray value is assigned as 98. The surrounding pixels that are more prominent than 98 is assigned as 1 otherwise it is assigned as 0 which infers the features are not predictable. The decimal value of the 11100011 is estimated as follows:

1 × 27 + 1 × 26 + 1 × 25 + 0 × 24 + 0 × 23 + 0 × 22 + 1 × 21 + 1 × 20, 1 × 128 + 1 × 64 + 1 × 32 + 0 × 16 + 0 × 8 + 0 × 4 + 1 × 2 + 1 × 1 = 227.

The micro pattern of the CXR image is obtained with the MB-LBP descriptors is highly useful in recognizing COVID-19 image. The hybrid MB-LBP local descriptors reduce the noises and the little scale components are accumulated form the large-scale operators.

WLD feature extraction

The histogram of the given image provides data about the position and shape. The WLD contains two components for generating the histogram of the image are differential excitation (μ) and orientation (ϕ). WLD algorithm consists of eight sequential steps that are described in Table 1. Figure 4 shows the process of WLD feature extraction.

Differential Excitation: The current pixel change (ΔDm) is estimated using the difference between the current (Dm) and neighboring pixels of the image (Dn). The current pixel differential excitation is Dn is estimated by the filter $f00$.

$$E_s^{00} = \sum_{m=0}^{p-1}(\Delta D_m) = \sum_{m=0}^{p-1}(D_m - D_n)$$

The i-th neighbor of the Dn is denoted as D_m $(m = 0, 1, \ldots . p - 1)$. The two filters output such as $f00$ and $f01$ is combined to find the ratio of the current pixel intensity and is estimated as follows:

$$H_R(D_n) = \frac{E_S^{00}}{E_S^{01}}$$

Table 1. WLD feature extraction algorithum.

Input: CXR image **Output:** WLD features
Step 1: Initialization WLD algorithm is employed for generating the histogram of the image and the input image.
Step 2: Compute the arctangent Function.
Step 3: Compute Differential Excitation.
Step 4: Compute gradient orientation.
Step 5: Mapping For orientation ϕ is quantized regarding performing the mapping
Step 6: Compute K dominant orientation ξk is calculated using the equation.
Step 7: Construct the concatenated histogram.
Step 8: Output: The WLS feature vectors WLD $(\mu i, \xi i)$ are produced.

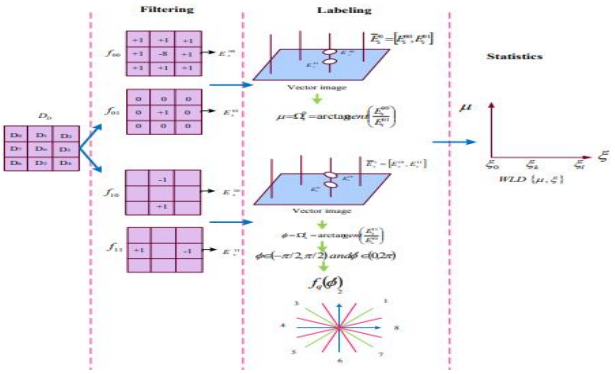

Figure 4. Computation of WLD descriptor.

ICA Feature reduction

ICA is the popular statistical feature reduction method which correlates the set of observed correlated variables to a set of values of linearly uncorrelated variables with the aid of orthogonal transformation. Furter, ICA is a non-linear extension of the PCA algorithm that uses kernel methods to learn the non-linear manifolds. ICA introduces the kernel which is used to map the higher dimension and original dimension of the features in the CXR image. ICA doesn't compute the principal components itself instead it projects the input data onto the element directions.

ICA is viewed as a broad view of the PCA which can able to minimize both higher and second order dependencies in the given input. Meanwhile, PCA decorrelates data only based on the second order statistic. ICA discovers the independent components by exploiting the statistical independence of the expected components. Two definitions exist in the independence for ICA algorithms are Minimization of Mutual Information (MMI) and Maximization of Non-Gaussian.

DLCNN Classifier

It has been developed in order to overcome the issues that have arisen with both deep learning and machine learning technologies. It is one of the most powerful approaches in the machine learning

paradigm, and it is used in many applications. There are a number of different DLCNN techniques that may be used to handle the covid-19 categorization challenges that exist. The suggested DLCNN model is shown in Figure 5.

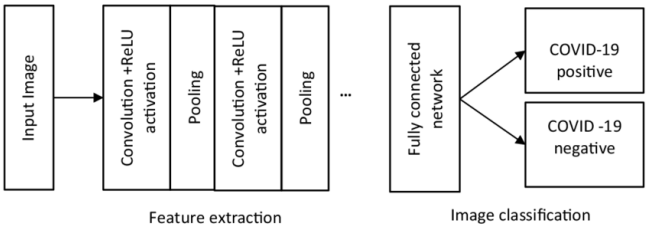

Figure 5. DLCNN based DR classification

Convolution Layer with learnable filters: This layer employs a collection of learnable filters that are used to identify the presence of particular characteristics or patterns that were present in the original CXR image. For a gaussian envelope, a convolution filter has a kernel size of 31*31 and a standard deviation of 5.0, which is the size of the kernel in a convolution filter.

Feature map pooling: This layer is used to execute down sampling, which acts separately on each feature map in order to shrink the supplied input CXR image in terms of spatial resolution. The MAX procedure is used to resize the CXR image after it has been captured. Additionally, pooling is subdivided into two types: MAX pooling and Average pooling. MAX pooling is the most common kind of pooling.

To learn convolution features, the convolution unit is utilised in combination with the Fully connected layer, which is used to learn disease-dependent properties from the CXR image. It is necessary to detect the highest amount of information possible in the raw CXR images' dynamic range, thus the kernel size and stride of the convolution are set to 3*3 and 1, respectively, to achieve this. The following layers are totally connected: It connects every neuron in one layer with every neuron in another layer, and it does so at the cellular level. A weight matrix is applied to the input CXR image, and then the bias vector is added in order to classify the image into the COVID-19 category.

RESULTS AND DISCUSSION

This work is concerned with the in-depth examination of the simulation findings, which is implemented by using MatlabR2021a. Furthermore, the proposed method's performance is compared to that of the current approaches utilising a variety of qualitative metrics.

Dataset

Three independent datasets were combined to create the second collection of CXR images, and they are all publicly accessible [31]. They are as follows: (1) COVID-19 CXR image dataset [32] (Colorado X-ray dataset). (2) Data from the Radiological Society of North America (RSNA) [33] is used. (3) The Montgomery County X-ray series from the United States National Library of Medicine (USNLM) [34]. There were a total of 2295 CXR CXR images in the dataset at the time of the tests (1583 normal CXR images and 712 COVID-19 images), and these images were utilized in this study.

Subjective performance

(a)

(b)

Figure 6. Classified outcomes (a) COVID-19, (b) Normal.

Figure 6, shows the classified outcomes by using proposed method. The random CXR images are classified as COVID-19 and normal classes.

Objective performance

Table 2. Performance comparison

Metric	SVM [17]	KNN [15]	RF [18]	Proposed
Accuracy	76.450	80.278	86.413	93.240
Sensitivity	76.836	79.307	90.480	93.557
Specificity	88.221	88.932	90.317	95.173
F1-Score	87.009	89.115	90.942	93.625
Precision	88.932	91.048	91.913	95.173
MCC	90.942	91.903	93.067	95.663

Here, SVM [17], KNN [15], and RF [18] are examples of existing approaches, that are compared to the efficacy of the proposed methodology in Table 2. According to the results of the simulations, the proposed COVID-19 classification technique outperformed all current methods for all metrics when compared to the existing approaches.

CONCLUSION

This article is focused on advanced artificial intelligence-based DR classification system. The proposed computer aided detection method is capable of classifying the DR at early stage. As a result, this technique identifies several features from DR using HOG, LBP, and LGDEP descriptors. Further, these are formed as hybrid features from the IDRID dataset. Then, LDA is used to select the best features from the hybrid features. Then, using these feature characteristics, a DLCNN model is trained to classify DR grades for each test retinal image. The simulation findings reveal that the proposed DR classification results outperform traditional methods in terms of subjective and object performance. This system can be extended with bio-optimization approaches for feature selection process.

REFERENCES

A Tiwari, Arti, Shilpa Srivastava, and Millie Pant. "Brain tumor segmentation and classification from magnetic resonance images: Review of selected methods from 2014 to 2019." Pattern Classification Letters 131 (2020): 244-260.

[1] Rinesh, S., [1]. "Investigations on Brain Tumor Classification Using Hybrid Machine Learning Algorithms." Journal of Healthcare Engineering 2022 (2022).

[2] Liu, Xingbin, Wenbo Mei, and Huiqian Du. "Multi-modality medical image fusion based on image decomposition framework and nonsubsampled shearlet transform." Biomedical Signal Processing and Control 40 (2018): 343-350.

[3] Yin, Haitao. "Tensor sparse representation for 3-D medical image fusion using weighted average rule." IEEE Transactions on Biomedical Engineering 65.11 (2018): 2622-2633.

[4] Dinh, Phu-Hung. "A novel approach based on grasshopper optimization algorithm for medical image fusion." Expert Systems with Applications 171 (2021): 114576.

[5] Parvathy, Velmurugan Subbiah, and Sivakumar Pothiraj. "Multi-modality medical image fusion using hybridization of binary crow search optimization." Health care management science 23.4 (2020): 661-669.

[6] Subbiah Parvathy, Velmurugan, Sivakumar Pothiraj, and Jenyfal Sampson. "A novel approach in multimodality medical image fusion using optimal shearlet and deep learning." International Journal of Scanning Systems and Technology 30.4 (2020): 847-859.

[7] Yang, Yong, [1]. "Multimodal medical image fusion based on fuzzy discrimination with structural patch decomposition." IEEE journal of biomedical and health informatics 23.4 (2018): 1647-1660.

[8] Jin, Xin, [1]. "Brain medical image fusion using l2-norm-based features and fuzzy-weighted measurements in 2-D Littlewood–Paley EWT domain." IEEE Transactions on Instrumentation and Measurement 69.8 (2019): 5900-5913.

[9] Liu, Feiqiang, [1]. "Medical image fusion method by using Laplacian pyramid and convolutional sparse representation." Concurrency and Computation: Practice and Experience 32.17 (2020): e5632.

[10] Li, Bo, [1]. "Medical image fusion method based on coupled neural p systems in nonsubsampled shearlet transform domain." International Journal of Neural Systems 31.01 (2021): 2050050.

[11] Zhu, Zhiqin, [1]. "A phase congruency and local Laplacian energy based multi-modality medical image fusion method in NSCT domain." IEEE Access 7 (2019): 20811-20824.

[12] Yin, Ming, [1]. "Medical image fusion with parameter-adaptive pulse coupled neural network in nonsubsampled shearlet transform domain." IEEE Transactions on Instrumentation and Measurement 68.1 (2018): 49-64.

[13] Liu, Yu, [1]. "Medical image fusion via convolutional sparsity based morphological component analysis." IEEE Signal Processing Letters 26.3 (2019): 485-489.

[14] Ganasala, Padma, and Achanta Durga Prasad. "Medical image fusion based on laws of texture energy measures in stationary wavelet transform domain." International Journal of Scanning Systems and Technology 30.3 (2020): 544-557.

[15] Li, Qiaoqiao, [1]. "Medical image fusion using segment graph filter and sparse representation." Computers in Biology and Medicine 131 (2021): 104239.

[16] Ding, Zhaisheng, [1]. "Brain medical image fusion based on dual-branch CNNs in NSST domain." BioMed research international 2020 (2020).

[17] Hu, Qiu, Shaohai Hu, and Fengzhen Zhang. "Multi-modality medical image fusion based on separable dictionary learning and Gabor filtering." Signal Processing: Image Communication 83 (2020): 115758.

[18] Kong, Weiwei, Qiguang Miao, and Yang Lei. "Multimodal sensor medical image fusion based on local difference in non-subsampled domain." IEEE Transactions on Instrumentation and Measurement 68.4 (2018): 938-951.

[19] Shehanaz, Shaik, [1]. "Optimum weighted multimodal medical image fusion using particle swarm optimization." Optik 231 (2021): 16641

[20] Ghosh, Sourodip, Aunkit Chaki, and K. C. Santosh. "Improved U-Net architecture with VGG-16 for brain tumor segmentation." Physical and Engineering Sciences in Medicine 44.3 (2021): 703-712.

[21] Zhang, Jinjing, [1]. "Brain tumor segmentation of multi-modality MR images via triple intersecting U-Nets." Neurocomputing 421 (2021): 195-209.

[22] Zhang, D., Huang, G., Zhang, Q., Han, J., Han, J., & Yu, Y. (2021). Cross-modality deep feature learning for brain tumor segmentation. Pattern Classification, 110, 107562.

[23] Zhou, Xinyu, [1]. "ERV-Net: An efficient 3D residual neural network for brain tumor segmentation." Expert Systems with Applications 170 (2021): 114566.

[24] Zhang, Wenbo, [1]. "ME-Net: Multi-encoder net framework for brain tumor segmentation." International Journal of Scanning Systems and Technology 31.4 (2021): 1834-1848.